Earth Syst. Sci. Data, 7, 87–92, 2015
www.earth-syst-sci-data.net/7/87/2015/
doi:10.5194/essd-7-87-2015

Open Access Earth System Science Data

Measurement of the fracture toughness of polycrystalline bubbly ice from an Antarctic ice core

J. Christmann[1], R. Müller[1], K. G. Webber[2], D. Isaia[2], F. H. Schader[2], S. Kipfstuhl[3], J. Freitag[3], and A. Humbert[3]

[1]Institute of Applied Mechanics, Technische Universität Kaiserslautern, 67663 Kaiserslautern, Germany
[2]Institute of Materials Science, Technische Universität Darmstadt, 64287 Darmstadt, Germany
[3]Glaciology section, Alfred-Wegener-Institut, Helmholtz Zentrum für Polar- und Meeresforschung, 27570 Bremerhaven, Germany

Correspondence to: J. Christmann (jchristm@rhrk.uni-kl.de)

Received: 18 July 2014 – Published in Earth Syst. Sci. Data Discuss.: 30 September 2014
Revised: 16 February 2015 – Accepted: 18 March 2015 – Published: 11 May 2015

Abstract. The critical fracture toughness is a material parameter describing the resistance of a cracked body to further crack extension. It is an important parameter for simulating and predicting the breakup behavior of ice shelves from the calving of single icebergs to the disintegration of entire ice shelves over a wide range of length scales. The fracture toughness values are calculated with equations that are derived from an elastic stress analysis. Additionally, an X-ray computer tomography (CT scanner) was used to identify the density as a function of depth. The critical fracture toughness of 91 Antarctic bubbly ice samples with densities between 840 and 870 $\mathrm{kg\,m^{-3}}$ has been determined by applying a four-point bending technique on single-edge v-notched beam samples. The examined ice core was drilled 70 m north of Kohnen Station, Dronnning Maud Land (75°00′ S, 00°04′ E; 2882 m). Supplementary data are available at doi:10.1594/PANGAEA.835321.

1 Introduction

In order to simulate and predict the calving of icebergs or the disintegration and breakup of ice shelves, the deformation and stress states within ice shelves need to be identified and related to material properties. Both, deformation and stress states, vary with location within an ice shelf. Therefore, knowledge of material data is crucial for numerical simulations. Depending on the timescale under consideration, one has to distinguish the material response of ice as viscous or elastic. In the long term, ice reacts like a viscous fluid. Frequently, a material model according to Glen is used, in which the important parameters are the shear viscosity and stress exponent; see Glen (1958) and Greve and Blatter (2009). On the other hand, the elastic response is valid on short timescales and the relevant parameters are fracture and rupture. The measurement of fracture toughness is performed at high deformation rates in order to trigger the brittle response of ice. In this measurement regime the theory of linear elastic fracture mechanics can be applied, ignoring the viscous and plastic properties of ice; see Schulson and Duval (2009). Traditionally, polar ice is assumed to be isotropic and therefore requires the knowledge of Young's modulus and Poisson's ratio. With an awareness of these model parameters, simulations can be performed. Additionally, measured velocity fields can be used to compute the strain and stress state locally.

For linear elastic materials the stress intensity factor (SIF) determines the criticality of a crack due to mechanical loading on the basis of macroscopic behavior; it therefore predicts the stress intensity around the tip of the crack. The reason for this is that, in a linear elastic model, the stress field is singular at the crack tip; thus, stress-based criteria fail to describe crack growth. In the presence of cracks, there are three different possibilities for further crack opening. Mode I describes symmetric crack opening perpendicular to the direction of the largest tensile stress. Mode II characterizes the sliding fracture mode, causing shear stresses, and mode III denotes the tearing mode. In all loading cases, the asymptotic behavior is given by the SIFs, usually denoted by K_{I}, K_{II} or K_{III}. For details on fracture mechanical concepts and the different fracture modes; see Gross and Seelig (2011). The SIF depends on the loading, the elastic material properties and the boundary conditions (geometry) under consideration. Once the SIF is known, it is compared to a critical fracture toughness value K_{Ic}, where we restrict attention to Mode I crack scenarios, as they typically represent the worst-case loading condition. For ice, the fracture toughness is influenced by many factors, such as density, grain size, temperature, microstructure, water content and salt content. Thus, it is experimentally challenging to measure fracture toughness. There are different techniques to measure the Mode I fracture toughness of a material such as three- and four-point loaded beams with a notch; see, for example, Goodman and Tabor (1978), Timco and Frederking (1982), Wei et al. (1991), Weber and Nixon (1996a) and Weber and Nixon (1996b) for seawater and freshwater ice. Furthermore, different parameters which have an influence on the critical fracture toughness are analyzed in Nixon and Schulson (1987), Nixon (1988), and Nixon and Schulson (1988) for tensile bars with a peripheral notch. Previous investigations on the fracture toughness of marine and glacier ice are found in Rist et al. (1999). These results are used as reference values in the present investigation.

Mechanical testing was performed in the ice lab at the Alfred-Wegener-Institut in Bremerhaven. The experimental setup was designed and built at the Institute of Materials Science at the Technische Universität Darmstadt.

The fracture toughness for ice cores from Antarctica has, to date, been tested with two experimental setups. Rist et al. (1996) utilized a three-point bend geometry for a chevron-notched round-bar specimen; this was used to perform experiments on Antarctic ice from one ice core. Rist et al. (1999) determined the critical stress intensity factor dependency on the density and porosity, also using a short-rod specimen geometry. The results from 18 different core samples were presented, in which controlled crack growth was obtained. The tests cover densities from 560 to 871 $\mathrm{kg\,m^{-3}}$. For the case of ceramics, Rice (2000) states that there is no unique method to measure the fracture toughness of a given material. According to the ASTM standards, several experimental setups are possible. In this investigation the ASTM standard for a four-point bending technique on single-edge v-notched beam samples was applied to ensure plane strain conditions. The measured parameters, which determine the fracture toughness, are assumed to be independent of the geometry and the loading situation. The advantage of this method is that the measured data of Sect. 2.2 (load-deflection curves) are not sensitive to small changes in the alignment of the ice sample. In addition, the fracture toughness measurements show a high amount of repeatability, verifying the insensitivity to geometry variations.

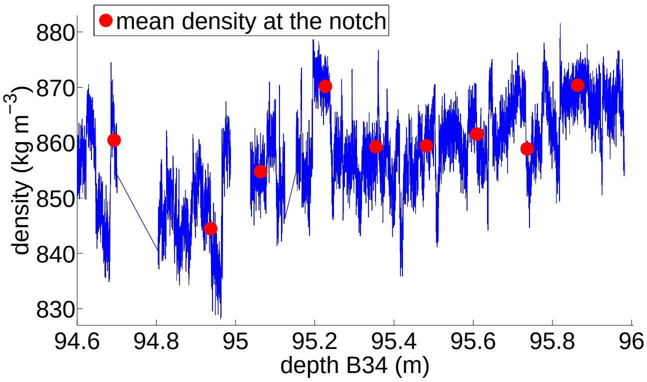

Figure 1. Depth–density profile of the ice core part considered.

2 Experimental methodology

2.1 Sample preparation

Bar-shaped samples for fracture testing were obtained from the B34 ice core, originally from a depth of between 94.6 m and 96 m. This core was drilled at Kohnen station (75°00′ S, 00°04′ E; 2882 m) on the East Antarctic plateau, a site of low accumulation rates and temperatures. Prior to testing, an X-ray microfocus computer tomograph (ICE-CT) was used to determine the density as a function of depth with a high vertical resolution, as shown in Fig. 1. Freitag et al. (2013) postulate that the variability of the density measurements, using two-dimensional X-ray scans, is less than other previously used methods as the noise level is lower. During analysis each 1 m long ice core was weighed to estimate the mean density from the ratio of weight to volume; this is the so-called volumetric method. This density is used as a calibration parameter for the two-dimensional X-ray scans. Regions of anomalies, conditioned by, for example, breaks or notches in the ice, are automatically detected and removed; see the missing parts in Fig. 1. For a detailed description of the construction and practical application of such an X-ray scan; see Freitag et al. (2013). The density profile shows that for greater depth the density increases slightly, whereas the density variability decreases, including standard deviations ranging from 5.15 to 9.25 $\mathrm{kg\,m^{-3}}$. The ice core was then cut into 12.6 cm long cylinders. The average density of the middle section of each disc, near the location of the fracture notch, was characterized; this is shown as red circles in Fig. 1. The accurate position of the notch was determined by taking into account the material loss due to the cutting process and the loss of waste ice. The mean density was calculated as an average, considering 2 cm of the surrounding density values.

Antarctic ice from an ice core was chosen, as we intended to have a sample that best represents the ice in situations to which the observational data will be applied (e.g., simulations of ice-shelf crack evolution). Artificially created samples would neither contain the impurities found in nature nor

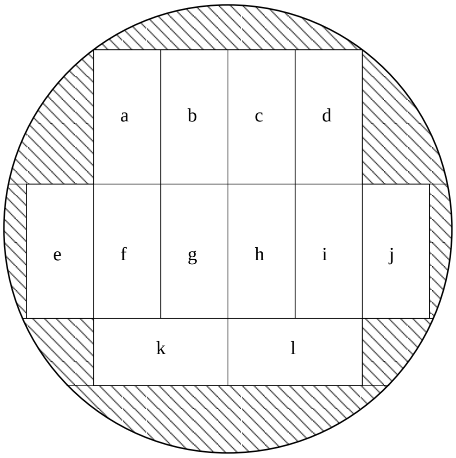

Figure 2. Cross section of ice core showing the sample location pattern.

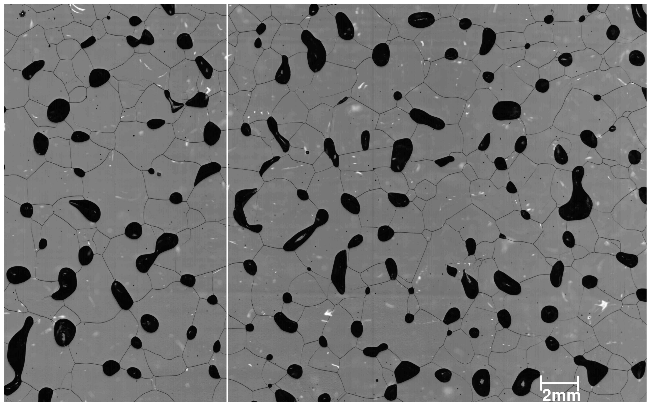

Figure 3. Representative microstructure of the B34 ice core showing air bubbles (black inclusions), grain boundaries (black lines) and the white line indicating where the grain size was measured.

would it represent the grain size distribution. As the porosity of the material, and hence the density, is the key parameter that determines the critical fracture toughness, the sample selection was performed by choosing a suitable density range. As the main aim was to increase the estimations of K_{Ic} at specific densities with sufficient statistics, one part of the ice core with nearly constant density was selected in order to obtain a large amount of samples. This could in future be extended by performing the same experiments with samples of other densities.

Because the aim was not to obtain the fracture toughness over a wide range of densities, representative of breaking ice shelves, ice from just below the firn–ice transition at a depth of 88 m (Freitag et al., 2013) was used. The accumulation rate at Kohnen Station is 65 mm of water equivalent (WE) or ≈ 72 mm of ice. A 12.6 cm long bar contains the accumulation of almost 2 years. The accumulation on ice shelves is generally much higher, with $> 200\,\mathrm{mm\,a^{-1}}$ WE and up to more than 500 mm.

Therefore, during the testing of the critical fracture toughness, it was important to minimize the density variation between samples. For this purpose, the core was cut into 9 cylinders with 12 samples each. Each cylinder was a 12.6 cm long section, resulting in samples cut at a 1.4 m depth interval for the B34 ice core. The ice core had a radius of $r = 50$ mm. Thus the experiments could be performed with 12 samples with nearly identical mean densities. The bar-shaped samples were cut with a band saw at $-20\,^{\circ}\mathrm{C}$ from the B34 ice core. Figure 2 shows a schematic cross section of an ice core with the sample location pattern. The location of the sample in one cross section of the ice core had no identifiable influence on the measured critical fracture toughness. Each specimen had a final thickness $W = 14.30$ mm, a width $B = 27.55$ mm and a length $L = 126$ mm. The width B of the sample is important to ensure that the crack tip is in a state of plane strain. This is proportional to the critical fracture toughness value and the inverse of the material's yield stress. In order to maximize the plane strain condition, within the possibilities given by the ice core geometry, B was taken to be larger than W to ensure that the crack face cut through a minimum of six grains. As part of the widely accepted ASTM standards, the crack length-to-sample height ratio should ideally be between 0.25 and 0.65. Ratios outside of this window introduce very minor errors due, in part, to the proximity of the crack tip plastic zone to the sample edge. In this study, however, due to the very low fracture toughness of ice, the crack was shortened slightly to increase the maximum force P_{max} required to cause failure. It was expected that a higher value would help reduce error or premature breakage during sample handling. Due to the nature of the preparation process the sample thickness and width were found to vary, with a standard deviation of 0.16 and 0.27 mm, respectively. The minor variations in sample size were not found to influence the fracture toughness measurements. Prior to testing, a notch was milled into each sample with a custom-built milling machine to ensure repeatability. The milling procedure was performed at $-15\,^{\circ}\mathrm{C}$, and a notch of approximately 2.5 mm depth was cut into each sample. The final notch radius was approximately $r_{\mathrm{a}} \approx 100\,\mu\mathrm{m}$, which was determined by the fixed radius of the cutting tool. Following the milling procedure, the cutting tool was analyzed with a light microscope with 100x magnification and the radius of the tool tip was determined. Although, it is known that the notch radius can influence the observed fracture toughness values, depending on the material's grain size; see Nishida et al. (1994); Rist et al. (2002) found that the grain size has no effect on the fracture toughness of ice at different depths of the Ronne Ice Shelf.

Figure 3 shows a representative microstructure of the tested ice. It is apparent that there is a distribution of grain sizes as well as significant porosity, indicated by the dark regions. The grain size was determined along the white line, which extends along the entire length of the sample

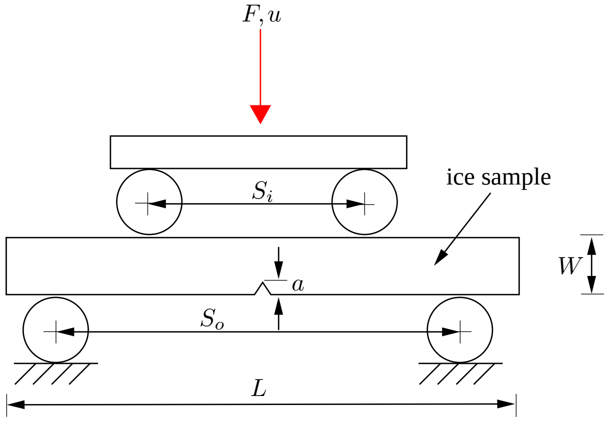

Figure 4. Schematic of four-point bending arrangement used to determine the critical fracture toughness.

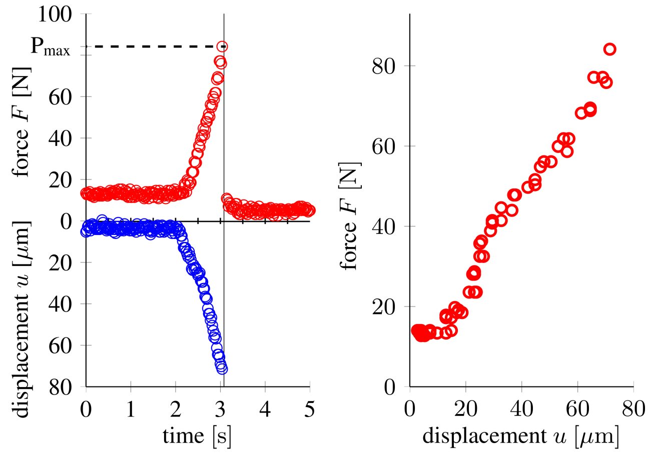

Figure 5. Representative central load and load-point displacement data as a function of time during a fracture experiment. The vertical thin black line represents the time at failure.

and represents approximately 90 grains. The measured mean grain size was found to be 1.15 mm, with a minimum and maximum observed grain size of 0.05 and 4.58 mm. The standard deviation was determined to be 0.81 mm along this line. The grain size was not found to vary in other analyzed sample sections, indicating that the stated grain size distribution is representative of the investigated part of the B34 ice core.

2.2 Fracture toughness measurements

The fracture toughness K_I is a material parameter that is used to characterize a material's resistance to further crack growth where there is a preexisting flaw; this is important in understanding when a material or structure will fail. Flaws can consist of a crack, grain boundary, pore, or other microstructural defects inherent in imperfect materials. In the case of a linear elastic material, K_I also fully defines the stress fields at the crack tip, which are intensified due to the presence of a sharp crack. If it is assumed that the material fails at a particular stress, then a critical fracture toughness value K_Ic can be used to predict the level of external mechanical load required to grow a crack of a given length and orientation. There are three fracture modes that define different loading conditions. Mode I, often referred to as the opening mode, is found when the external load is applied perpendicular to the fracture surface. This loading condition occurs often and represents the worst-case scenario due to the relatively low fracture toughness values in comparison to Modes II and III, i.e., the most likely failure mode; see Gross and Seelig (2011).

There are various techniques available to determine the Mode I fracture toughness of a material; these rely on different experimental geometries. In the present investigation the K_Ic values of Antarctic ice were obtained at $-15\,^\circ$C using the four-point bending technique, shown schematically in Fig. 4. Due to the geometry of the experimental arrangement, the sample in the vicinity of the crack tip is in a state of pure bending, which results in a tensile stress at the crack tip. Experiments were carried out according to the ASTM (2008) E 1820-08 standard. During testing, each notched sample was monotonically loaded to failure with a displacement u and measured with a linear variable differential transformer (LVDT), which has a resolution of approximately ± 150 nm. The resultant mechanical load F was found to increase approximately linearly with the displacement and was measured by a load cell with a resolution of approximately ± 1 N (load cell data). The displacement, load and time were measured at a frequency of 50 Hz with a LabVIEW program.

Following sample preparation the ice sample was loaded to failure under displacement control with a rate of approximately $65\,\mu\mathrm{m\,s^{-1}}$, corresponding to a loading rate of $\sim 67\,\mathrm{N\,s^{-1}}$. Figure 5 displays representative force and displacement data as a function of time during a fracture experiment. It is apparent that both the displacement and force increase approximately linearly up to the point of fracture, defined as the maximum load prior to failure P_max. After this load is reached, the crack grows and the sample fractures, resulting in the force instantaneously decreasing. The critical fracture toughness of each sample was determined using the maximum measured force, the sample geometry and the positioning of the loading rollers. The equations to calculate the fracture toughness for pure bending are derived from an elastic stress analysis, and the results are given here:

$$K_\mathrm{Ipb} = K_\mathrm{Ic} = f(a/W)\left[\frac{P_\mathrm{max}[S_\mathrm{o} - S_\mathrm{i}]10^{-6}}{B W^{3/2}}\right]\left[\frac{3[a/W]^{1/2}}{2[1-a/W]^{3/2}}\right],$$

where

$$f = f(a/W) = 1.9887 - 1.326[a/W] - \frac{\{3.49 - 0.68[a/W] + 1.35[a/W]^2\}[a/W]\{1-[a/W]\}}{\{1+[a/W]\}^2},$$

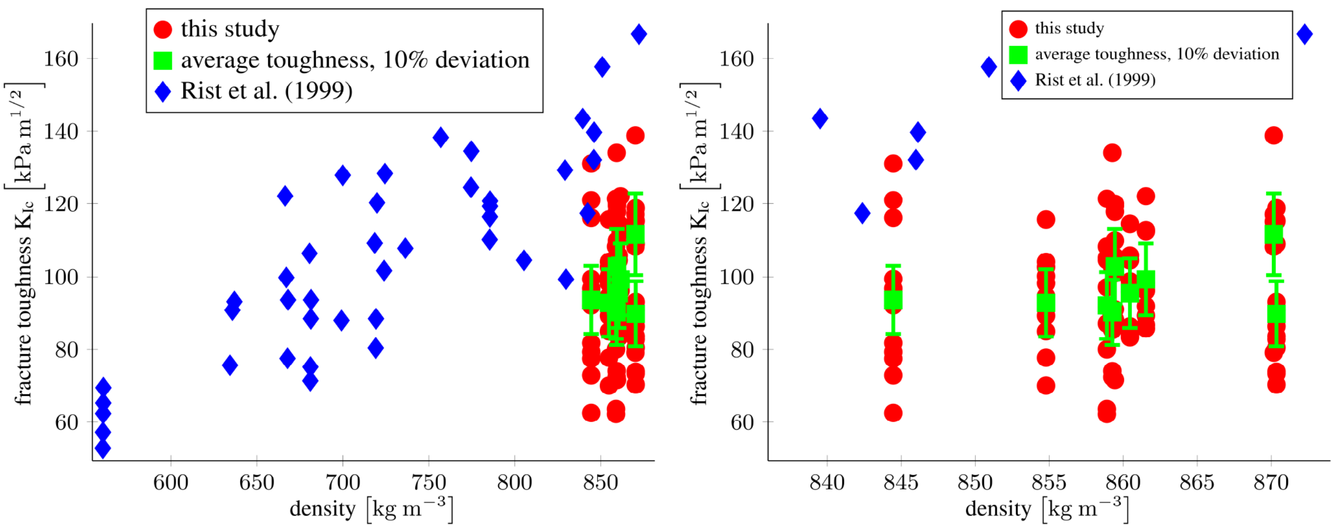

(a) (b)

Figure 6. **(a)** Comparison to results from Rist et al. (1999) and the average of the measured fracture toughness values. **(b)** Detail magnification of the measured range.

P_{max} is the maximum applied force, S_o the span of the outer rollers ($S_o = 102.8$ mm) and S_i the span of the inner rollers ($S_i = 51.4$ mm). The dimension B is perpendicular to the crack depth, W is the dimension parallel to the crack depth and a is the notch depth. For details see ASTM (2007).

3 Results and discussion

During experimental characterization, 108 samples were measured. Of these samples, 91 failed due to a crack emanating from the notch; the other samples broke at another position away from the notch, most likely due to a local defect that resulted in a higher stress intensity factor than at the notch. During analysis, only the samples that failed at the notch were used to calculate the fracture toughness. Wei et al. (1991) studied the influence of crack (or notch) radii for freshwater columnar ice produced with six different methods for single-edge notched-bend specimens and analyzed the impact of notch acuity. In this investigation, the average standard deviation was 33.95 % using a four-point bending experimental arrangement, which is comparable to the current setup. The average critical fracture toughness, shown based on our measurements, was found to be 95.35 kPa m$^{1/2}$, with an average standard deviation of $\pm$16.69 kPa m$^{1/2}$ for densities ranging from 844.5 to 870.3 kg m^{-3} (Fig. 6). In Fig. 6, each red circle represents an individual measurement; the average toughness for each density from the middle section of the nine cylinders (see Fig. 1) is depicted by green squares with error bars that correspond to a 10 % deviation. The new results derived for Antarctic inland ice are compared in Fig. 6 with the results obtained by Rist et al. (1999), shown as blue diamonds. The temperature of $-15\,^{\circ}$C was prescribed due to the conditions in the ice lab. Rist et al. (1999) measured the critical fracture toughness in an ice lab at $-20\,^{\circ}$C and stated "we believe that within experimental error, temperature would have no significant effect on our measured values of fracture toughness for shelf ice" (Rist et al., 1999). Therefore, it is possible to compare those results to the one obtained by the four-point bending technique presented here. It can be clearly observed that the critical stress intensity values from the results measured previously are approximately 30–50 % larger than the average values determined by the four-point bending experiments. This could be due to a higher loading rate, a larger notch radius or differences in the type of ice tested. The average standard deviation for a four-point bending technique is assumed in the literature to be between 2 and 7 % for homogeneous ceramics; see Gogotsi (2003). This spread will be much larger if the material is relatively heterogeneous or full of defects (like ice-core ice). The standard deviation of the critical fracture toughness for the current measurements was approximately 17.5 %. Nevertheless, the maximum absolute variation of 16.69 kPa m$^{1/2}$ for fracture toughness measurements of any sort is relatively small when compared to, for example, materials such as structural ceramics, where an absolute deviation of several MPa m$^{1/2}$ is possible; see Gogotsi (2003). The absolute value of the critical fracture toughness for ice, here 95.35 kPa m$^{1/2}$, is small compared to other materials, but the absolute distribution of 40 % is nevertheless significant. However, the larger number of samples tested, with a comparable distribution in the literature of critical fracture toughness variations for a given scattering for ice, demonstrates the repeatability of the current measurements. It should also be considered that (i) the measurements were performed on natural materials with various impurities and (ii) that a relatively small number of grains were tested in each sample due to the grain size. Both of these factors can lead to an increased sample-to-sample variation. Additionally, the investigation of the sample thickness, the sample width and the location of the sample reveal that their influence on the results were negligibly small.

4 Conclusions

The critical stress intensity factor was experimentally determined for bubbly ice from Antarctica. During testing, single-edge v-notch beam samples in a four-point loading configuration were utilized and monotonically loaded to failure. The investigated density range was too small to conclusively observe a density-dependent change in the fracture toughness. In total, 91 samples were investigated, allowing for the determination of an average critical stress intensity and a standard deviation, determined to be $95.35\,\mathrm{kPa\,m^{1/2}}$ and $\pm 16.69\,\mathrm{kPa\,m^{1/2}}$, respectively. Comparison to previous experimental results (Rist et al., 1999) shows good agreement, particularly when the variations in the ice sample and different testing conditions are considered. The samples are sawed and tested in only 3 days, and, due to the small dimension of a sample, the loss of material is minimized. The distribution of the critical fracture toughness was shown to be very small in comparison with other materials. In further research, the density interval should be extended by analyzing different depths in one or more drill cores. This would provide a better statistical evaluation of the possible critical fracture toughness values. Different locations, such as ice from Greenland firn cores with different impurities or regions where the ice is known to be more anisotropic, could give further indications of the possible variation in fracture toughness values.

Acknowledgements. This work was supportd by DFG priority program SPP 1158, project numbers HU 1570/5-1; MU 1370/7-1.

Edited by: D. Carlson

References

ASTM C1421-01b: Standard Test Methods for Determination of Fracture Toughness of Advanced Ceramics at Ambient Temperature, Annual Book of Standards, Vol. 15.01, ASTM International, West Conshohocken, doi:10.1520/C1421-10, 2007.

ASTM E1820-08: Standard Test Methods for Measurement of Fracture Toughness, Annual Book of Standards, Vol. 03.01, ASTM International, West Conshohocken, doi:10.1520/E1820, 2008.

Dempsey, J. P.: The fracture toughness of ice, Ice-Structure Interaction, IUTAM Proceeding, Springer-Verlag, Berlin Heidelberg, 109–145, 1991.

Freitag, J., Kipfstuhl, S., and Laepple, T.: Core-scale radioscopic imaging: a new method reveals density-calcium link in Antarctic firn, J. Glaciol., 59, 1009–1014, 2013.

Gogotsi, G. A.: Fracture toughness of ceramics and ceramic composites, Ceramics International, 29, 777–784, 2003.

Goodman, D. J. and Tabor, D.: Fracture toughness of ice: a preliminary account of some new experiments, J. Glaciol., 21, 651–660, 1978.

Glen, J. W.: The flow law of ice, a discussion of the assumptions made in glacier theory, their experimental foundations and consequences, IAHS-AISH P., 47, 171–183, 1958.

Greve, R. and Blatter, H.: Dynamics of Ice Sheets and Glaciers, Springer, Berlin, 2009.

Gross, D. and Seelig, T.: Fracture Mechanics with an Introduction to Micromechanics, Springer, Berlin, 2011.

Nishida, T., Hanaki, Y., and Pezzotti, G.: Effect of notch-root radius on the fracture toughness of a fine-grained alumina, J. Am. Ceram. Soc., 77, 606–608, 1994.

Nixon, W. A.: The effect of notch depth on the fracture toughness of freshwater ice, Cold Reg. Sci. Technol., 15, 75–78, 1988.

Nixon, W. A. and Schulson, E. M.: A micromechanical view of the fracture toughness of ice, J. Phys., 48, 313–319, 1987.

Nixon, W. A. and Schulson, E. M.: Fracture toughness of ice over a range of grain sizes, J. Offshore Mech. Arct., 110, 192–196, 1988.

Rice, R. W.: Mechanical Properties of Ceramics and Composites: Grain and Particle Effects, Marcel Dekker, New York, 2000.

Rist, M. A., Sammonds, P. R., Murrell, S. A. F., Meredith, P. G., Oerter, H., and Doake, C. S. M.: Experimental fracture and mechanical properties of Antarctic ice: preliminary results, Ann. Glaciol., 23, 284–292, 1996.

Rist, M. A., Sammonds, P. R., Murrell, S. A. F., Meredith, P. G., Doake, C. S. M., Oerter, H., and Matsuki, K.: Experimental and theoretical fracture mechanics applied to Antarctic ice fracture and surface crevassing, J. Geophys. Res., 104, 2973–2987, 1999.

Rist, M. A., Sammonds, P. R., Oerter, H., and Doake, C. S. M.: Fracture of Antarctic shelf ice, J. Geophys. Res.-Sol. Earth, 107, ECV2-1–ECV2-13, 2002.

Schulson, E. M. and Duval, P.: Creep and Fracture of Ice, Cambridge University Press, Cambridge, 2009.

Timco, G. W. and Frederking, R. M. W.: Flexural strength and fracture toughness of sea ice, Cold Reg. Sci. Technol., 8, 35–41, 1982.

Weber, L. J. and Nixon, W. A.: Fracture toughness of freshwater ice – Part I: Experimental technique and results, J. Offshore Mech. Arct., 135–140, 1996a.

Weber, L. J. and Nixon, W. A.: Fracture toughness of freshwater ice – Part II: Analysis and micrography, J. Offshore Mech. Arct., 118, 141–147, 1996b.

Wei, Y., DeFranco, S. J., and Dempsey, J. P.: Crack-fabrication techniques and their effect on the fracture toughness and CTOD for fresh-water columnar ice, J. Glaciol., 37, 270–280, 1991.